Bubble-assisted Liquid Hole Multipliers in LAr

A. Tesi, E. Erdal, A. Breskin, D. Vartsky & S. Bressler

Dept. of Astrophysics & Particle Physics, Weizmann Institute of Science, Israel

RD51 meeting, CERN, October 22nd 2019

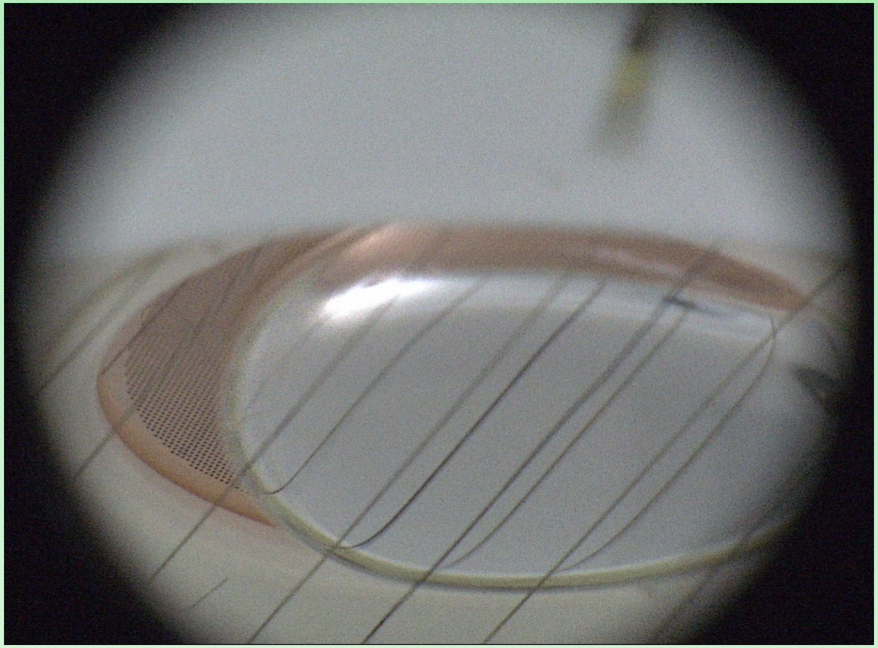

The concept – Detector geometry

- A CsI-coated perforated electrode (GEM, THGEM) is immersed in the noble liquid;
- A bubble in inflated using resistive wires and trapped underneath the electrode;
- A dedicated light readout (PMT, SiPM) is present below the wires.
- 3 electric fields:
  - E_d – Cathode-Top
  - E_{THGEM} – Top-Bottom
  - E_t – Bottom-Wires

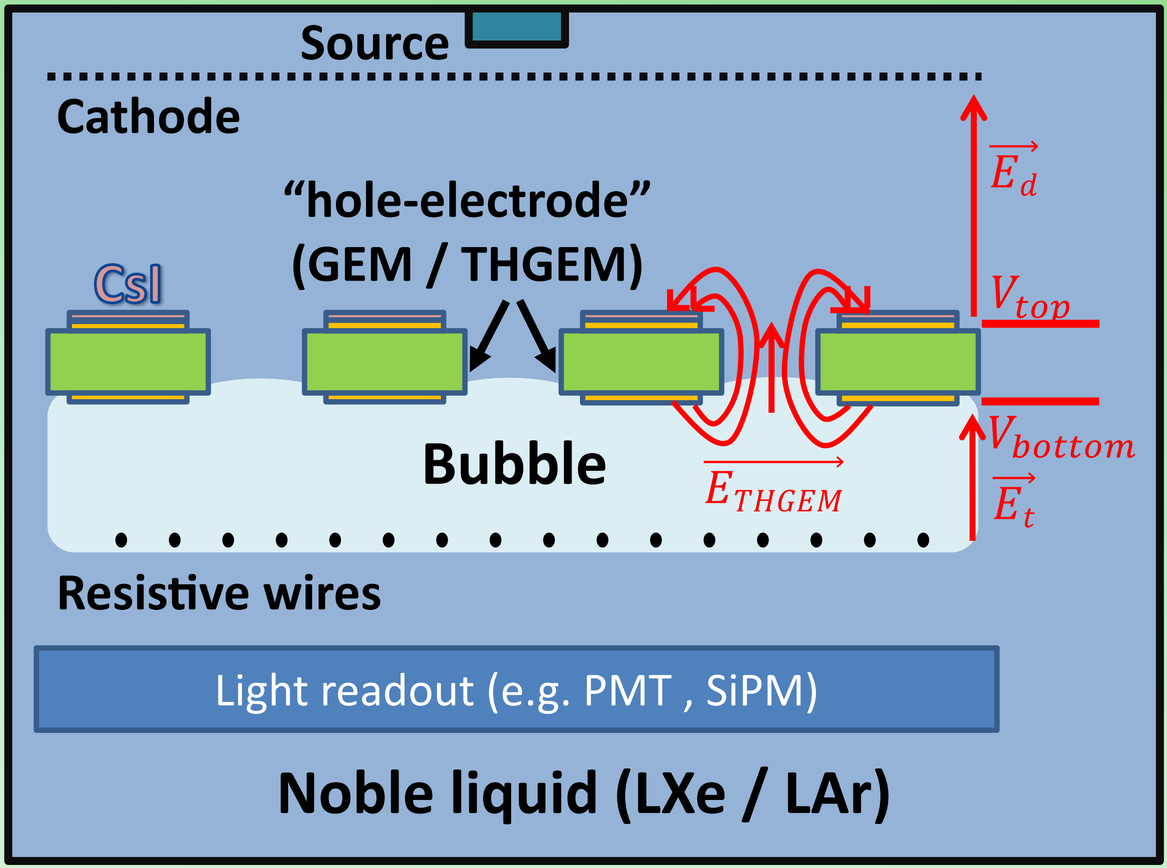

First Demo in LXe:

L. Arazi et al. 2015 *JINST* 10 P08015 [arXiv:1505.02316]

E. Erdal et al. 2015 *JINST* **10** P11002 [arXiv:1509.02354]

The concept – Physics

Radiation-induced electroluminescence
from a bubble trapped in noble liquid

- **S1** – Primary scintillation light due to de-excitation;
- **S1'** – Electroluminescence induced by a single photoelectron extracted from the photocathode;
- **S2** – Electroluminescence induced by ionization electrons extracted from the liquid and transferred into the gaseous phase towards the THGEM bottom.

Note that, <u>if E_t is implemented</u>, electrons can travel through the bubble reaching the wires.

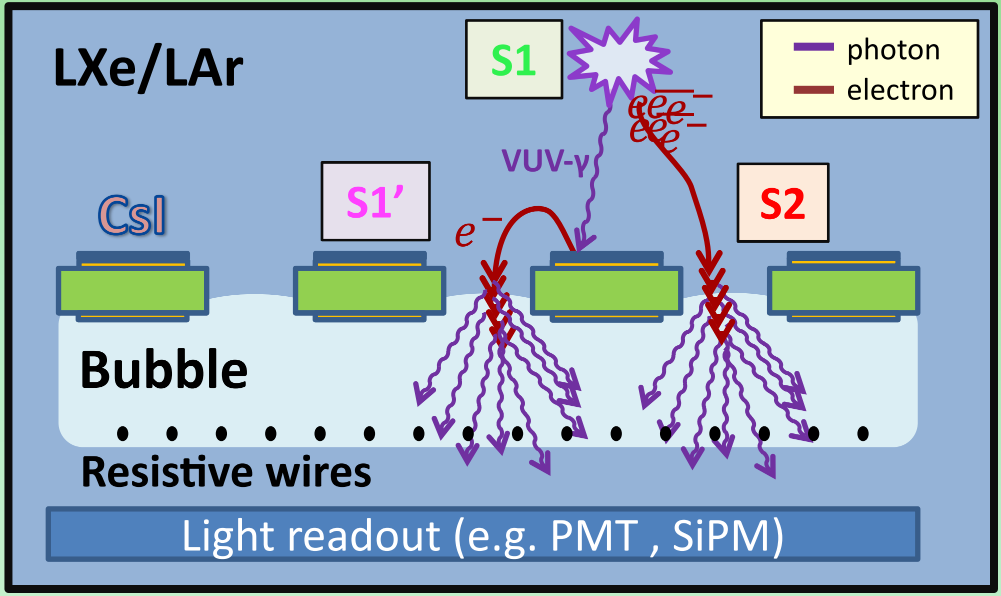

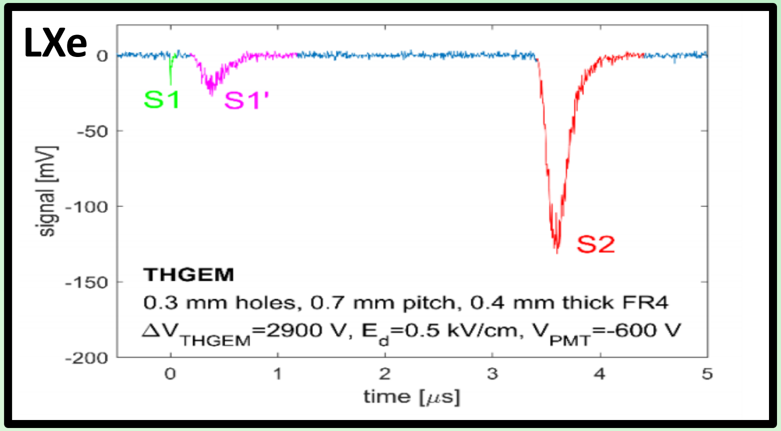

L. Arazi et al. 2015 *JINST* 10 P08015 [arXiv:1505.02316]
E. Erdal et al. 2015 *JINST* **10** P11002 [arXiv:1509.02354]

Previous results in LXe

- Successful operation as a charge and light readout. Light yield: **up to 400 photons/e/4π**
- Investigation of different geometries (THGEM/GEM/SC-GEM) - **SC-GEM: highest gain**
- Modest charge multiplication in the bubble in addition to EL - ~**8 for E_t~2-15 kV/cm**
- Very good **E_{RES} ~ 6% RMS with α**

  (~7000 primary e^- - no recombination, ~2000 VUV-induced pe^-)
- Imaging of an ^{241}Am source with pixelated (Quad-SiPM) readout - ***R_{xy} ~ 200µm RMS**

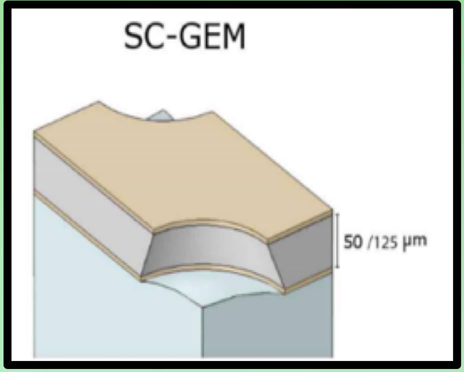

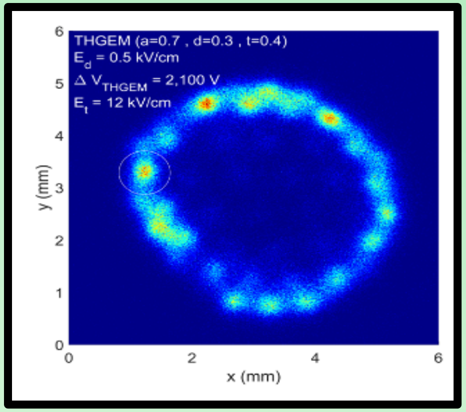

E. Erdal et al. 2015 JINST **10** P11002 [arXiv:1509.02354]
E. Erdal et al. 2018 *JINST* **13** P12008 [arXiv:1708.06645]
E. Erdal et al. 2019 *JINST* **14** P01028 [arXiv:1812.00780]

*R_{xy} = Position Reconstruction Resolution

Ar as a possible alternative to Xe

Technology of choice for neutrino and some dark-matter experiments (WArP, ArDM, DarkSide, DUNE)

- **Good medium**
  - *massive*
  - *high scintillation yield*
  - *good ionizer*
- **Much Cheaper than Xe and abundant**
  - large volumes are accessible! (DUNE ~ 68 Ktons Ar)
- **High-purity levels** : easy to achieve
- **PSD** : Good electron / nuclear recoil discrimination power (τ_1=5ns, τ_2=1.6μs)
- **Shorter WL** ➔ bare photo-sensors or with wavelength shifter (TPB)
- **Lower T** : ~90 °K

Element	Xenon	Argon
Atomic Number Z	54	18
Atomic mass A	131.3	40.0
Boiling Point T_b [K]	165.0	87.3
Liquid Density @ T_b [g/cm^3]	2.94	1.40
Fraction in Earth's Atmosphere [ppm]	0.09	9340
Price	$$$$	$
Scintillator	✓	✓
W_{ph} (α, β) [eV]	17.9 / 21.6	27.1 / 24.4
Scintillation Wavelength [nm]	178	128
Ionizer	✓	✓
W (E to generate e-ion pair) [eV]	15.6	23.6
Experiments [stopped, running, in preparation]	~ 5	~ 5

V. Chepel & H. Araujo 2013 *JINST* **8** R04001 [arXiv:1207.2292]
R. Acciarri & al. 2016 *FERMILAB-DESIGN-2017-02* [arXiv:1512.06148]

OUR CHALLENGE - Can we maintain a stable bubble in LAr and operate such a system as a detector?

WISArD – WIS Ar Detector

Currently tested configuration

^{241}Am, no CsI, windowless SiPM/TPB+PMT

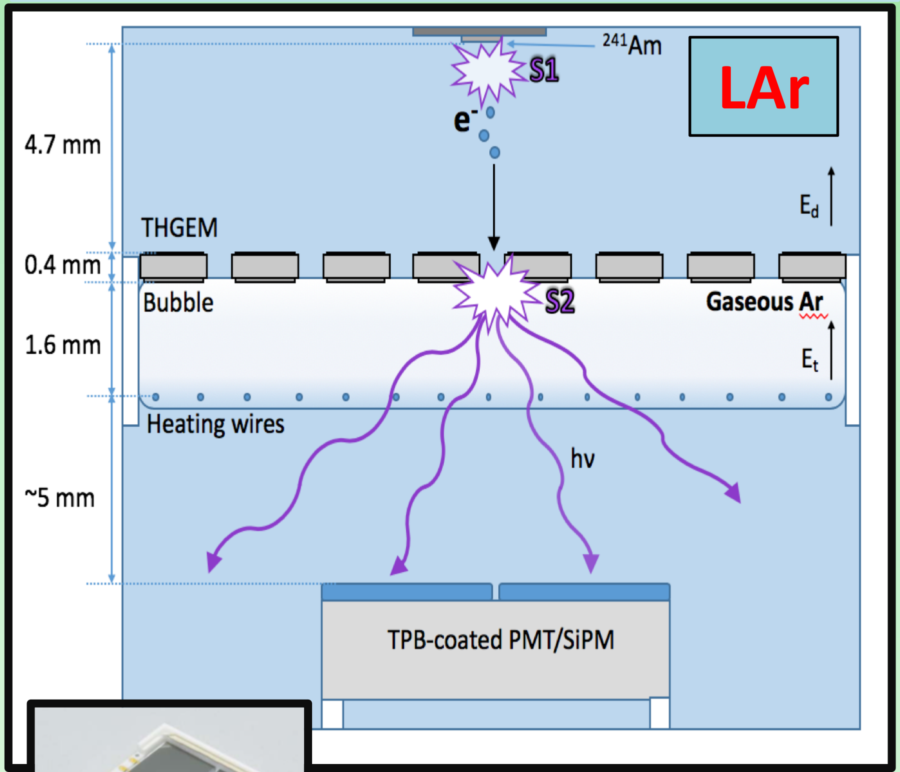

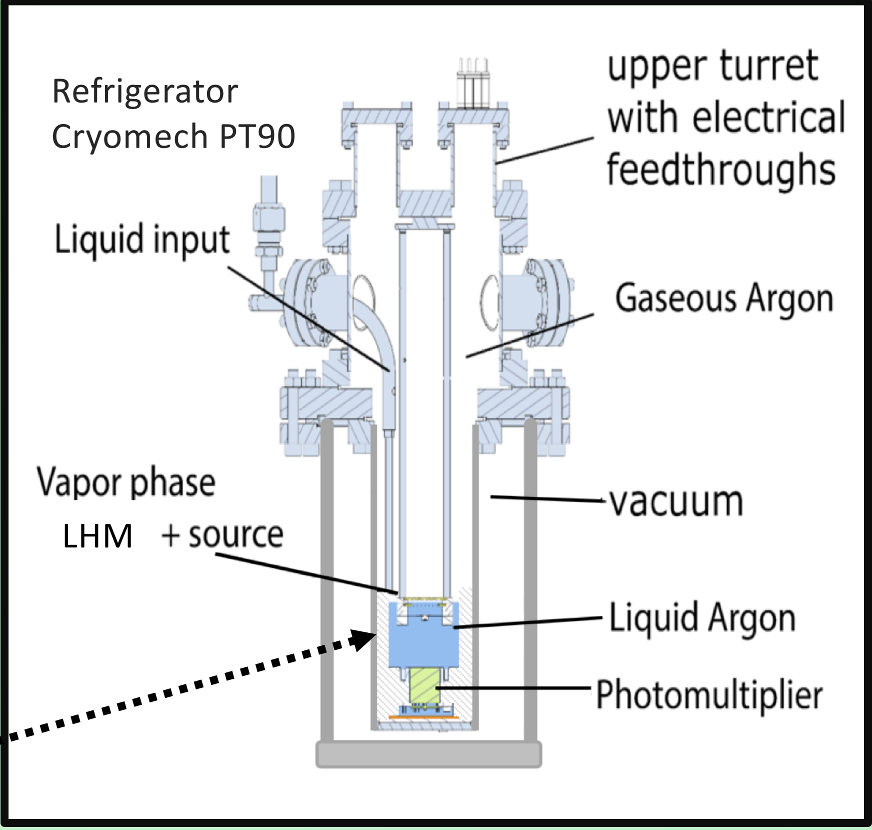

The cryostat

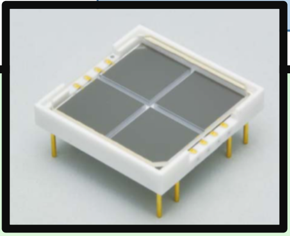

A four-elements windowless SiPM (Hamamatsu VUV4 MPPC S13371- 6050CQ-02, total area 12x12 mm^2)

Erdal et al. [arXiv:1908.04974] (submitted to JINST)

First results of LAr-LHM

First experimental proof that the bubble concept works also in LAr!!

No CsI on top of the THGEM: **S2 only**

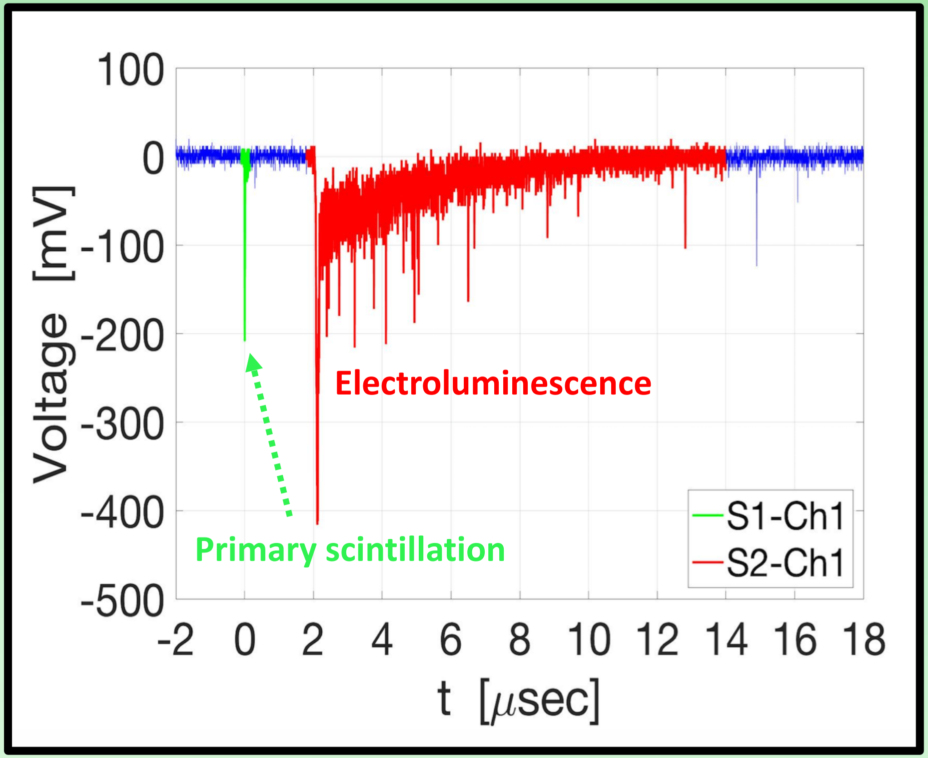

Example of alpha-particle induced single-event waveform, recorded by a TPB-coated PMT.

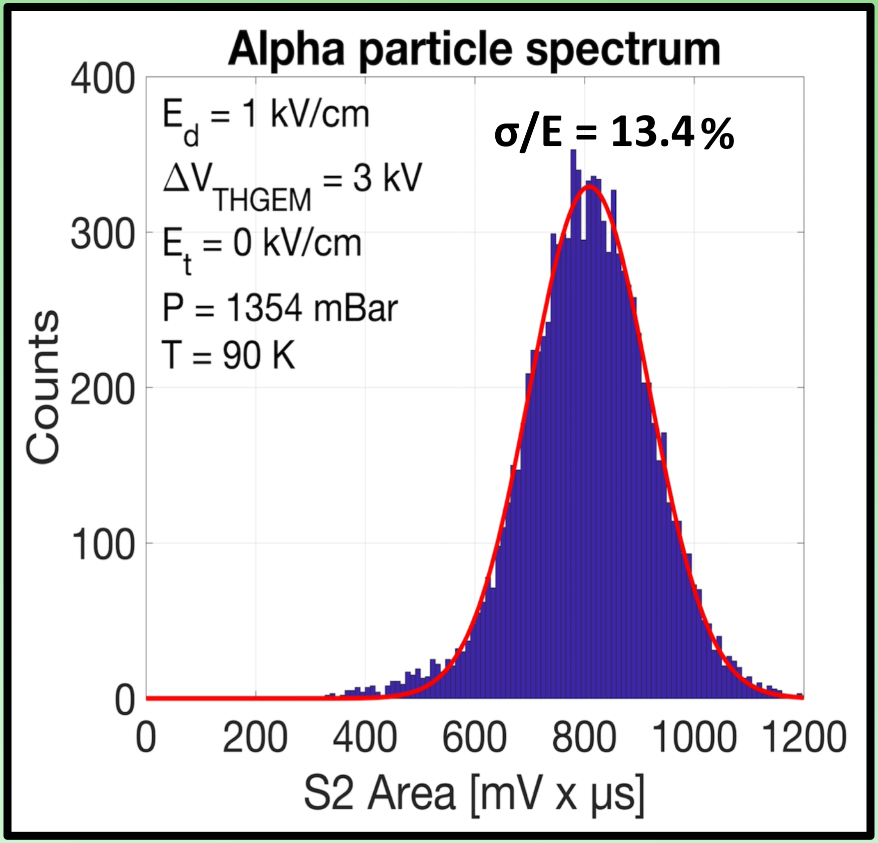

Erdal et al. [arXiv:1908.04974] (submitted to JINST)

Response of the LAr-LHM detector

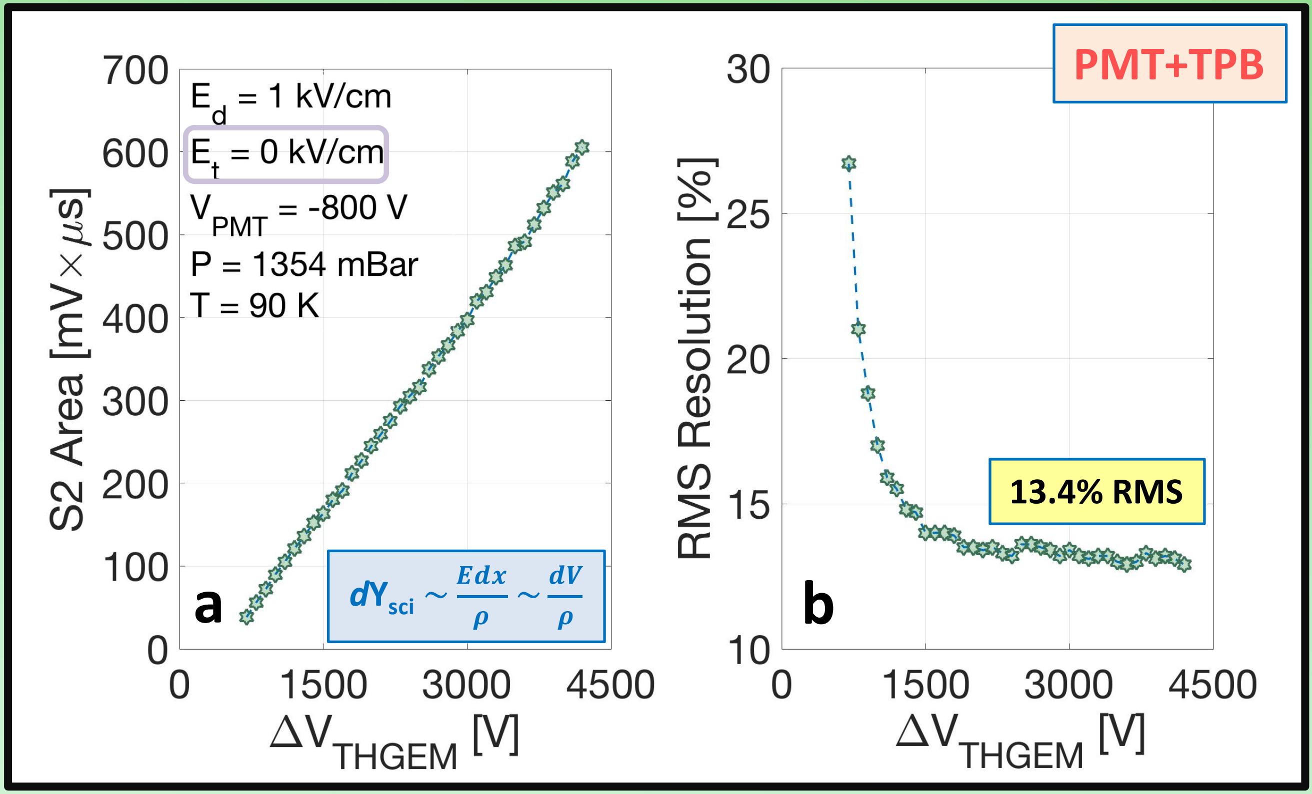

a) Pulse area vs voltage across the THGEM electrode. The linear trend ➔ EL without charge gain

b) RMS E_{Res} of the area distribution.

Procedure

- 10000 total events;
- For each waveform, computation of S2-pulse area + histogram;
- Gaussian fit of the histogram to derive mean value and resolution.

Windowless QUAD-SiPM: Similar response to PMT/TPB

Erdal et al. [arXiv:1908.04974] (submitted to JINST)

Q Multiplication in the transfer gap I

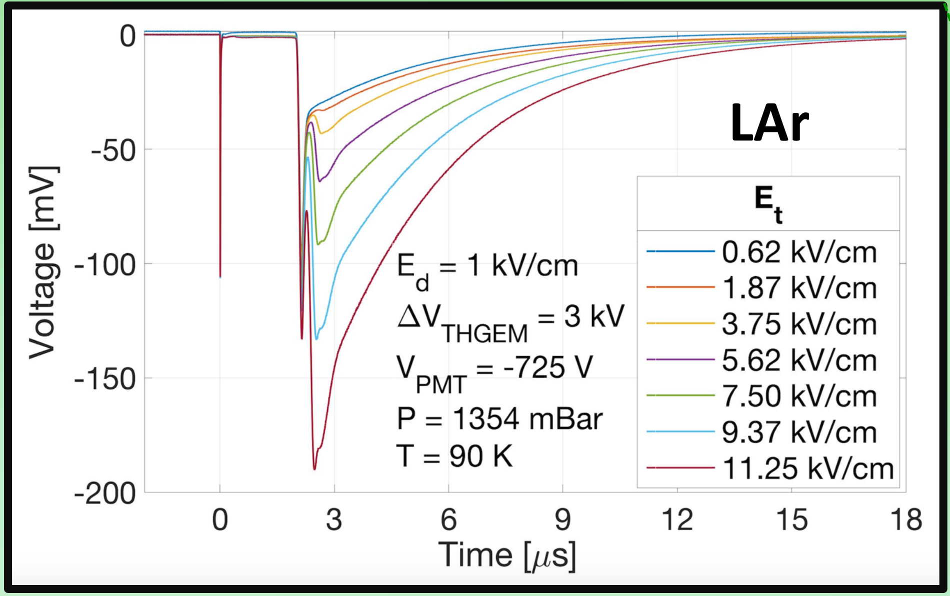

Average pulse-shapes vs E_t

- Significant increase in signal magnitude;
- Different shape - presence of a hump.

Setup with E_t implemented

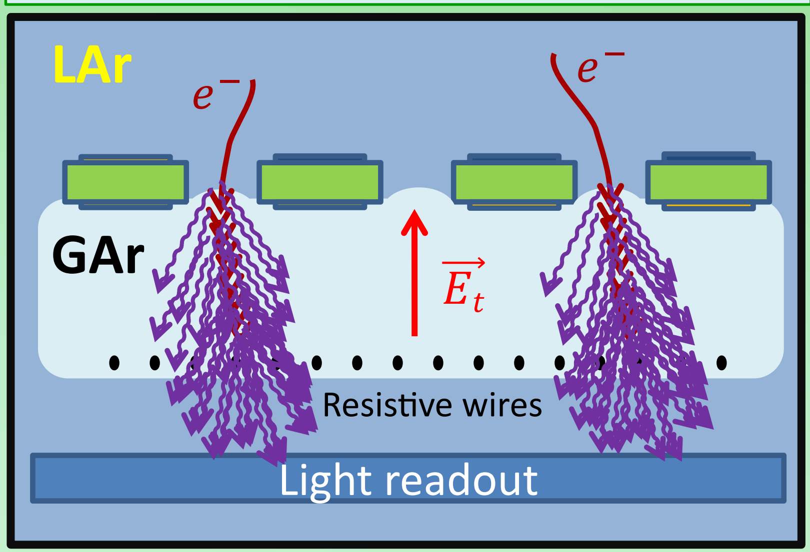

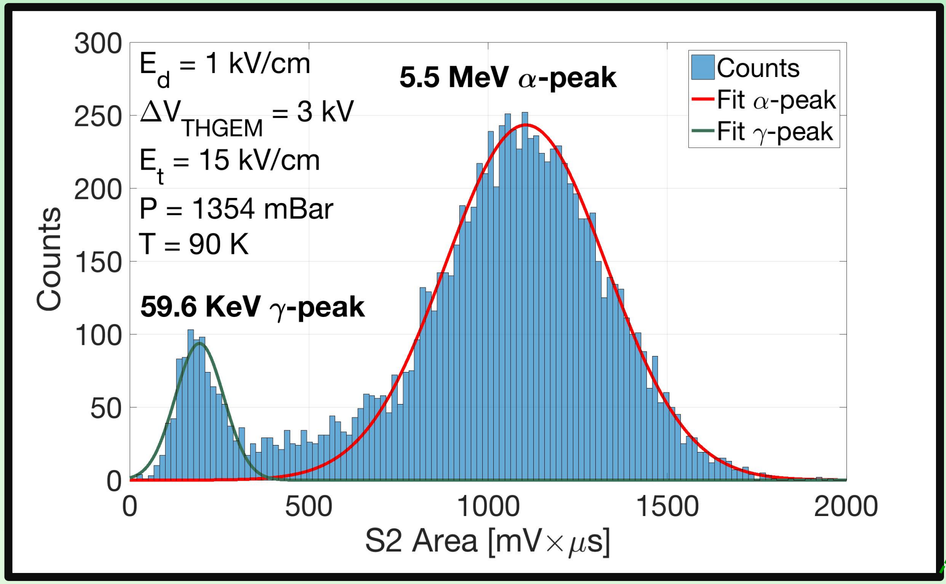

Pulse-area spectrum @ E_t = 15 kV/cm of 5.5 MeV Alpha particles & 59.5 keV gamma

Erdal et al. [arXiv:1908.04974] (submitted to JINST)

Q multiplication in the transfer gap II

Exponential charge multiplication vs E_t

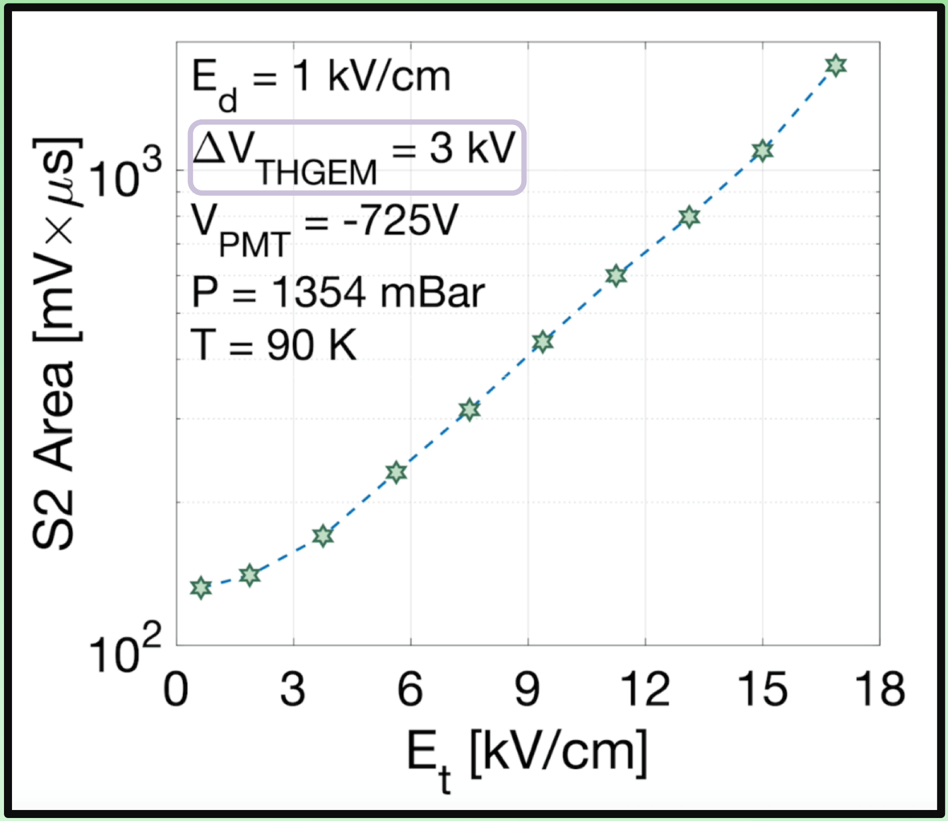

! – 'E_t' should be considered as «<u>indicative</u>» close to the wires.

@ **'E_t' < 2 kV/cm** ➔ linear increase in light yield (EL only)

@ **'E_t' > 2 kV/cm** ➔ charge multiplication onset nearby the heating wires

@ **'E_t' > 15 kV/cm** ➔ Intense charge multiplication – the photonic emission becomes visible in the spectrum.

S2 vs E_t – Above ~2 kV/cm, the pulse-area grows exponentially
➔ Charge multiplication ~10 for E_t~3-17 kV/cm.

Erdal et al. [arXiv:1908.04974] (submitted to JINST)

Imaging ^{241}Am source: LAr-LHM with Quad-SiPM

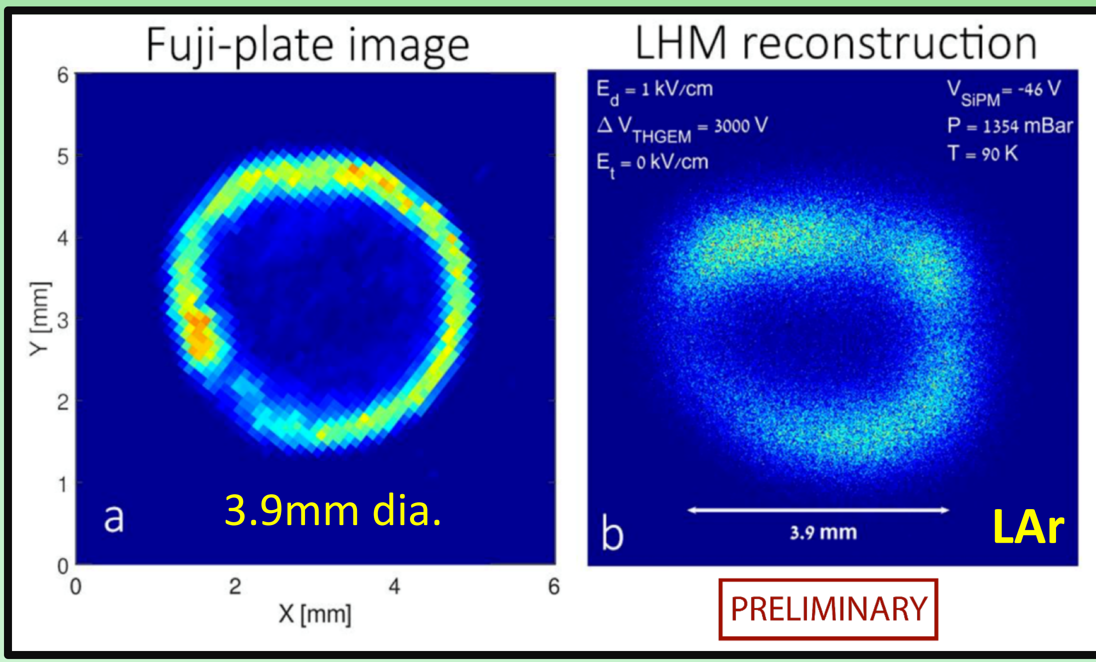

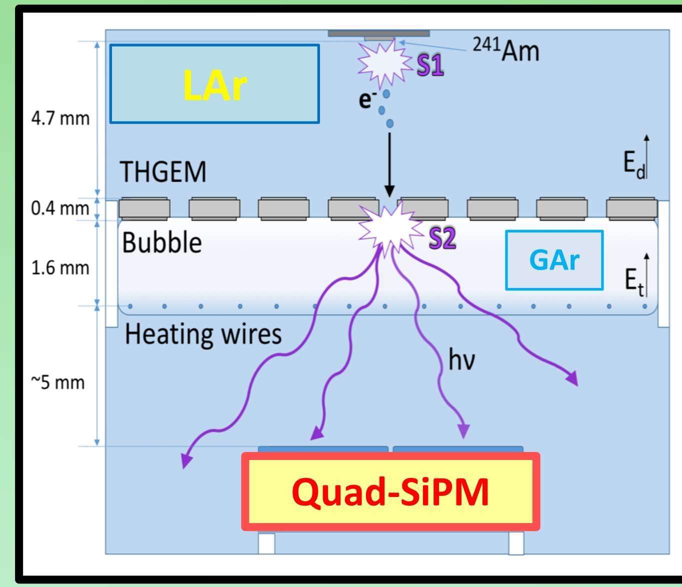

Sub-mm reconstruction resolution, with a simple center-of-gravity algorithm (very preliminary).

$$\vec{R} = \frac{A \cdot \sum L_i \cdot \vec{r}_i}{\sum L_i}$$

For comparison:

In **LXe-LHM:** $R_{XY} \sim 200$ µm

Preliminary – not optimized

In **LAr-LHM:** $R_{XY} \sim 600$ µm

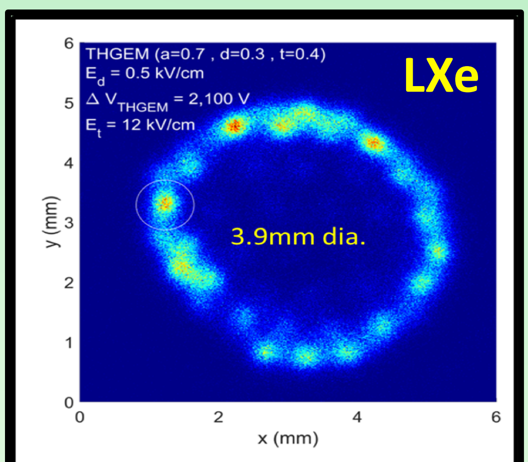

E. Erdal et al. 2019 *JINST* **14** P01028 [arXiv:1812.00780]

Summary

- We successfully demonstrated for the first time the operation of a bubble-assisted LAr-LHM;
- We conducted preliminary measurements of several properties – S2 Area vs ΔV_{THGEM}, vs E_t, E_{RES} and R_{XY} …
- We submitted a paper to JINST – *Erdal et al. [arXiv:1908.04974]*

Next steps – Two fronts

- Investigation and modeling of the underlying physical processes dictating the performance;
- Systematic characterizations.

The physics behind LAr-LHM

- **Bubble dynamics** – Formation, stability, shape of the liquid-to-gas interface, bubble penetration into the holes;
- **E_{RES}** – We observed a discrepancy (2-fold lower than in Xe). Why?
- **PDE** – In LXe we measured a 5-fold lower PDE of a CsI-coated electrode than the predicted one. Electron loss. Is this going to happen also in LAr-LHM?
- **Electron transfer efficiency** – How is it correlated to the liquid-to-gas interface? Does it affect E_{RES}?
- **Potential barrier from liquid-to-gas** – Does it play a role? (0.69eV in LXe vs 0.2eV in LAr)
- **R_{xy}** – We observed a difference (3-fold lower than in Xe). Why?

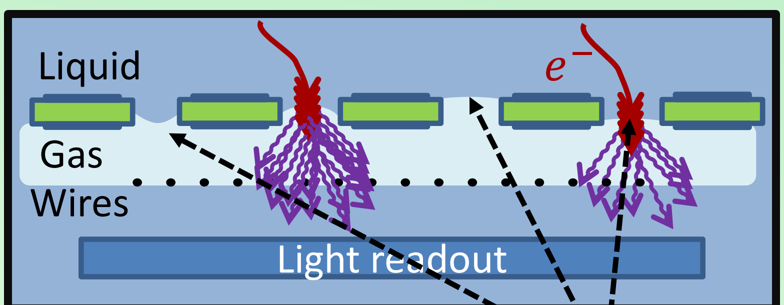

Interface shape?
Experimental and modeling R&D

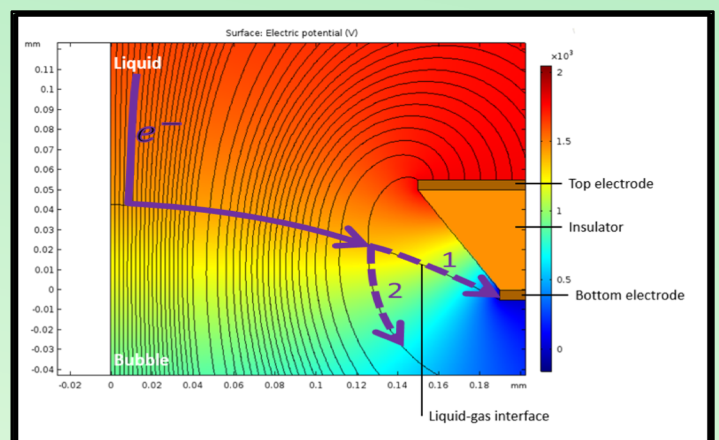

Systematic characterizations

- **Different electrode geometries** :

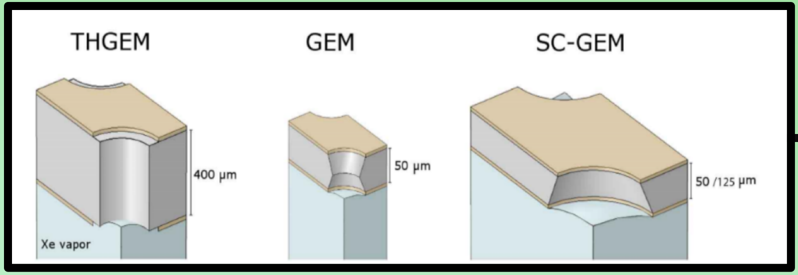

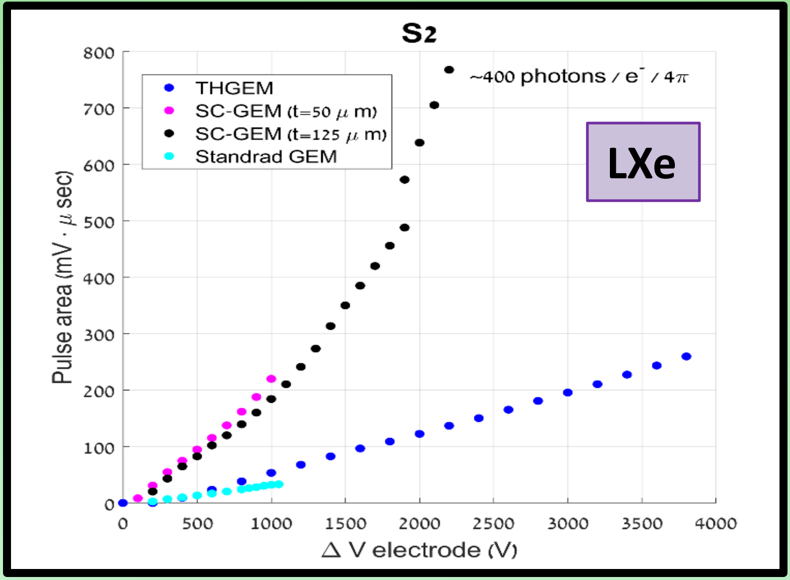

LXe-LHM: **SC-GEM best performance**
LAr-LHM: same trend?

- **Measurement of additional detector properties**
  - Absolute QE of CsI in LAr;
  - PDE;
- **Operation in depth –** Essential in large scale experiments;
- **Larger prototypes**

E. Erdal et al. 2018 *JINST* **13** P12008 [arXiv:1708.06645]

Thank you!

Backup slides

Liquid Argon features

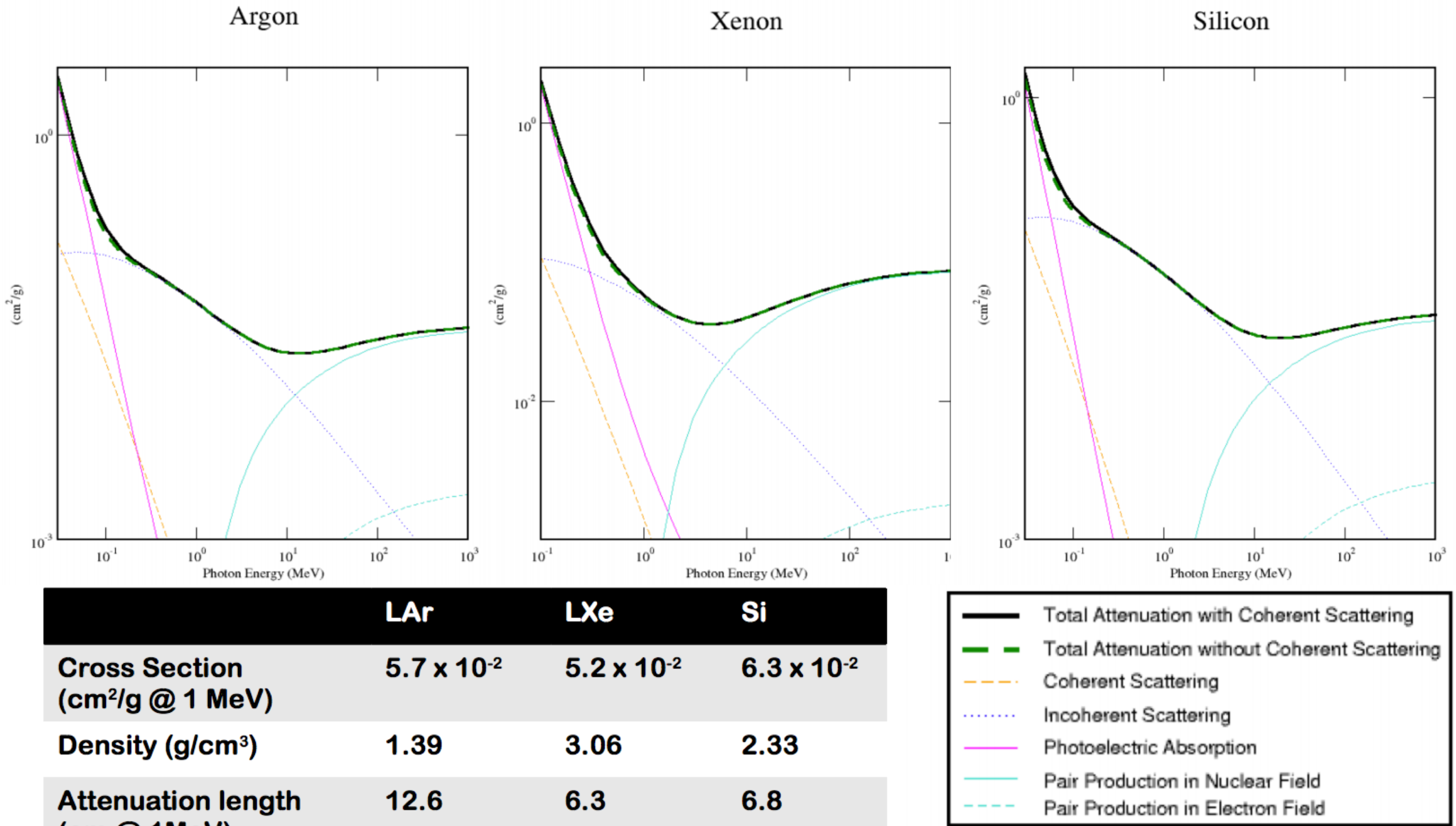

	LAr	LXe	Si
Cross Section (cm^2/g @ 1 MeV)	5.7×10^{-2}	5.2×10^{-2}	6.3×10^{-2}
Density (g/cm^3)	1.39	3.06	2.33
Attenuation length (cm @ 1MeV)	12.6	6.3	6.8
Radiation length	14.3	2.77	9.3

PSD

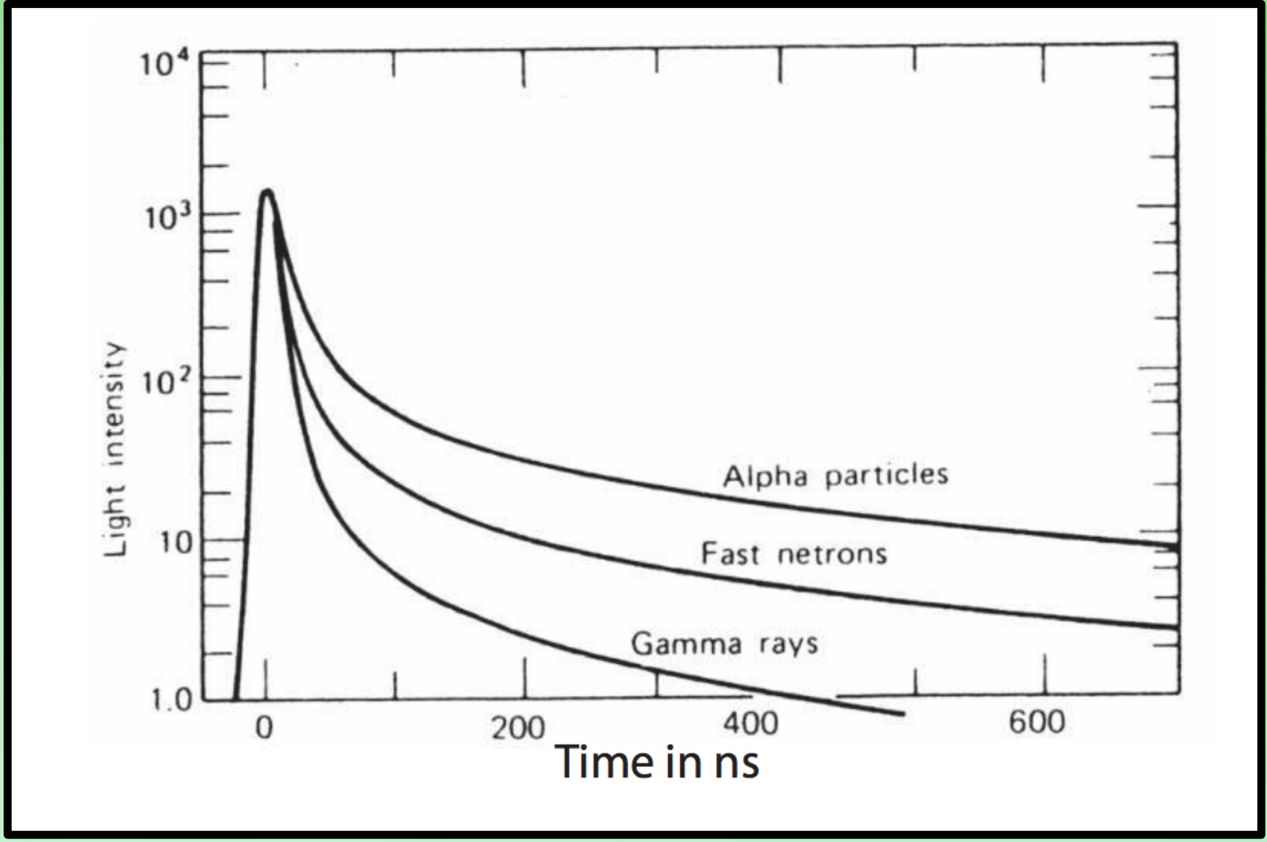

PSD rests on the difference of the relative intensities of the slow component, depending on the specific energy loss of the particle (dE/dx). In contrast to LAr, the relative intensities of the slow component increase with dE/dx. When particles present a large dE/dx, the density of excitons is higher along the track of the particles which results in increased bimolecular interactions between two excited states responsible for the delayed fluorescence. Therefore this type of interaction will increase the slow part in the scintillation light, allowing a PSD on the signal between neutron (proton recoils) and gamma (electron recoils).

Scintillation yield of LXe and LAr as a function of LET

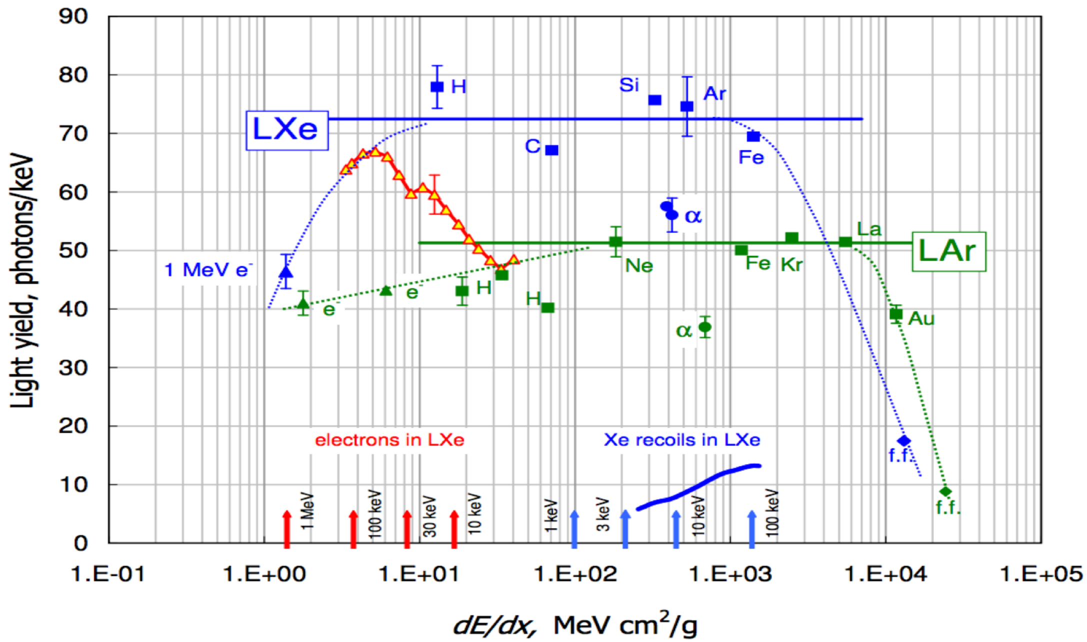

Figure 11. Scintillation yield of LXe and LAr as a function of linear energy transfer for various particles. Data points (in blue for LXe, and in green for LAr) are after [73] (figures 2, 4 and Table III); not all data points are shown for clarity. For the same reason, only a typical error bar is shown for each dataset. Dashed lines are for guiding the eye only, no underlying model is assumed; the top plateau corresponds to a minimum energy to produce a scintillation photon W_s^{min}=13.8 eV for LXe and 19.5 eV for LAr according to [63, 73]. Red arrows indicate average dE/dx values for electrons in LXe calculated as the initial particle energy (indicated next to arrow) divided by the range from ESTAR [121]; blue arrows indicate $(dE/dx)_e$ for Xe recoils in LXe calculated in a similar way using stopping power and range tables from SRIM [62] and the Lindhard partition function from [81]. The red yellow-filed triangles represent the relative measurements with Compton electrons reported in [60]; we re-scaled their energy to dE/dx using ESTAR as above, and re-normalized their response to that of γ-rays at ≈120 keV using the evaluated curve from [103] as in figure 10.

V. Chepel & H. Araujo 2013 *JINST* **8** R04001 [arXiv:1207.2292]

Probability of electron emission from liquid to gas as a function of electric field

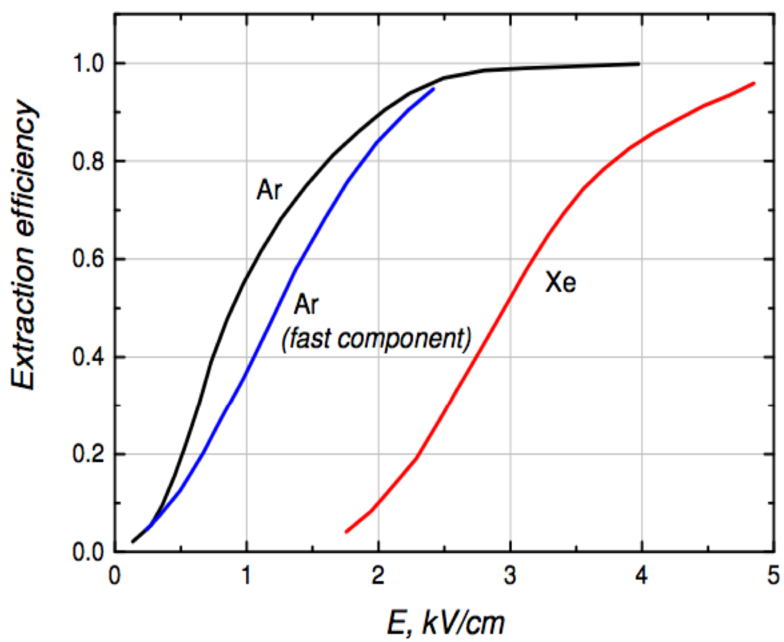

Figure 18. Probability of electron emission from liquid to gas as a function of electric field. Re-drawn from data in [207].

V. Chepel & H. Araujo 2013 *JINST* **8** R04001 [arXiv:1207.2292]

QE of reflective CsI photocathode in vacuum

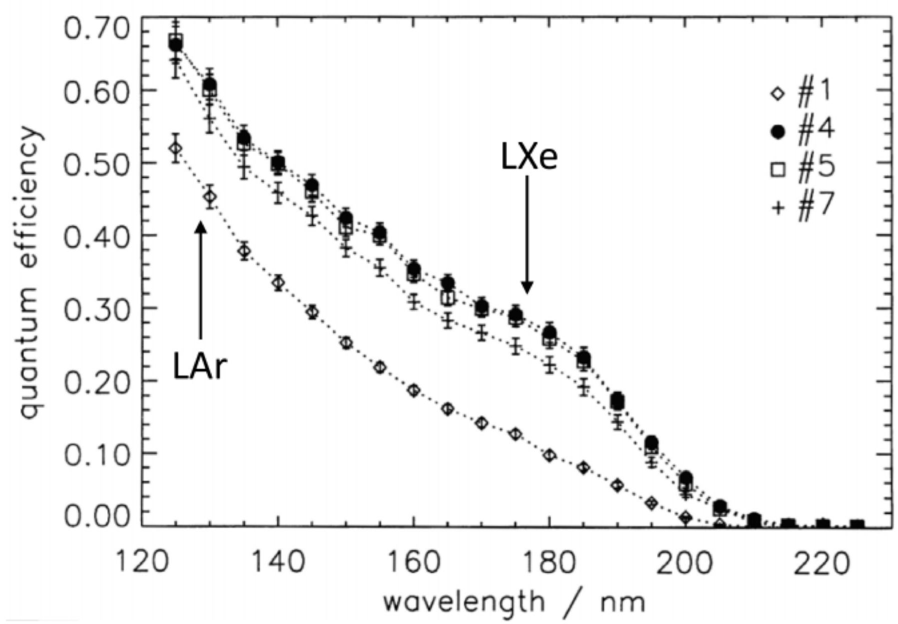

Figure 27. Quantum efficiency of reflective CsI photocathodes in vacuum as a function of the photon wavelength for four different samples. The arrows indicate the emission wavelengths for liquid argon and xenon. (Adapted from [330]; with permission from Elsevier.)

V. Chepel & H. Araujo 2013 *JINST* **8** R04001 [arXiv:1207.2292]

Scintillation and Ionization yield in LXe

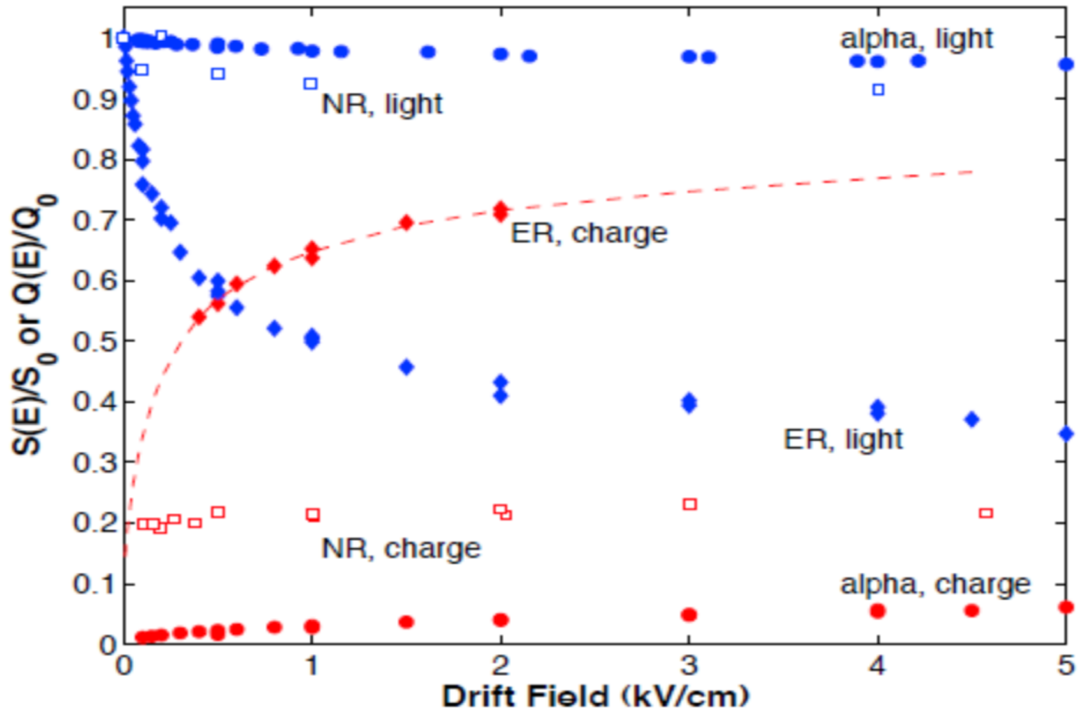

FIG. 6 Field dependence of scintillation and ionization yield in LXe for 122 keV electron recoils (ER), 56.5 keVr nuclear recoils (NR) and 5.5 MeV alphas, relative to the yield with no drift field (27).

E. Aprile & T. Doke 2010 Rev. Mod. Phys. **82**, 2053

Scintillation and Ionization yield in LAr

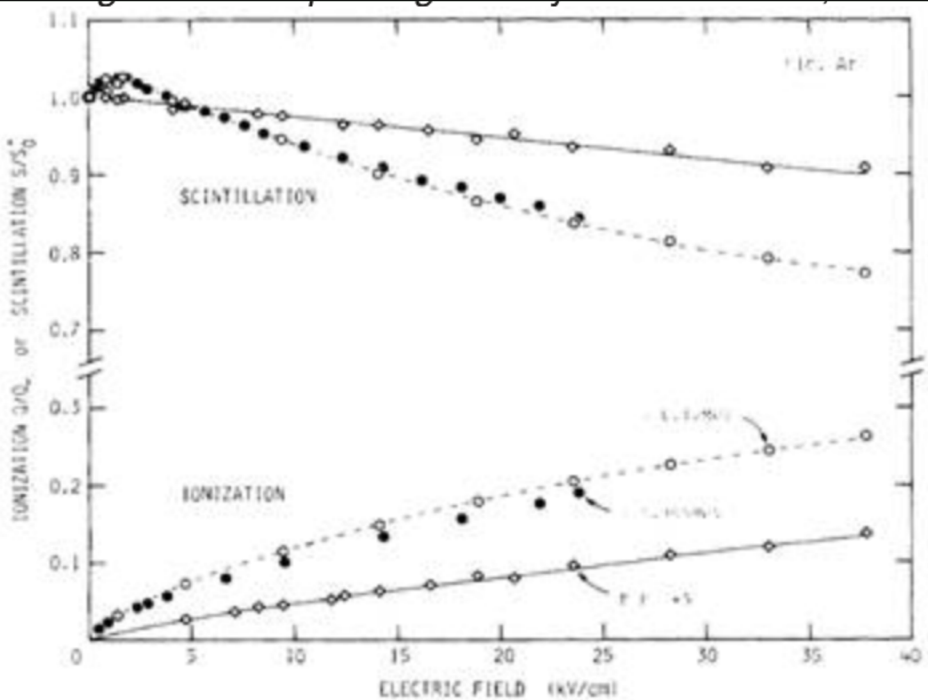

FIG. 1. Variation of the scintillation S and ionization Q yields for α particles (●, 5.305 MeV; ○, 6.12 MeV) and fission fragments (FF) (◇) in liquid argon as a function of applied electric field. S'_0 is the scintillation yield obtained at zero electric field, and Q_∞ is the charge produced by an ionizing particle.

Hitachi, A., et al., *Scintillation and ionization yield for α particles and fission fragments in liquid argon.* Physical Review A, 1987. **35**(9): p. 3956

Electrode specifications

	THGEM	Standard GEM	Single-conical GEM	Single-conical GEM
Insulator	FR4	polyimide	polyimide	polyimide
Thickness	0.4 mm	50 µm	50 µm	125 µm
Hole diameter(s)	0.3 mm	top/mid/bottom 70/50/70 µm	top/bottom 300/340 µm	top/bottom 300/400 µm
Hole pitch	1 mm	140 µm	600 µm	600 µm
Cu thickness	20 µm	5 µm	5 µm	5 µm
Hole rim	50 µm	--	--	--